*Korean J. Chem. Eng.*, 35(7), 1509-1516 (2018)
DOI: 10.1007/s11814-018-0037-5

pISSN: 0256-1115
eISSN: 1975-7220

# Conceptual feasibility studies of a $CO_X$-free hydrogen production from ammonia decomposition in a membrane reactor for PEM fuel cells

**Sehwa Kim, Jiseon Song, and Hankwon Lim†**

Department of Advanced Materials and Chemical Engineering, Catholic University of Daegu,
13-13 Hayang-ro, Hayang-yep, Gyeongsan, Gyeongbuk 38430, Korea
(*Received 11 July 2017 • accepted 22 February 2018*)

**Abstract**−$CO_X$-free hydrogen production from ammonia decomposition in a membrane reactor (MR) for PEM fuel cells was studied using a commercial chemical process simulator, Aspen HYSYS®. With process simulation models validated by previously reported kinetics and experimental data, the effect of key operating parameters such as $H_2$ permeance, He sweep gas flow, and operating temperature was investigated to compare the performance of an MR and a conventional packed-bed reactor (PBR). Higher ammonia conversions and $H_2$ yields were obtained in an MR than ones in a PBR. It was also found that He sweep gas flow was favorable for $X_{NH_3}$ enhancement in an MR with a critical value (5 kmol $h^{-1}$), above which no further effect was observed. A higher $H_2$ permeance led to an increased $H_2$ yield and $H_2$ yield enhancement in an MR with the reverse effect of operating temperature on the enhancement. In addition, lower operating temperature resulted in higher $X_{NH_3}$ enhancement and $H_2$ yield enhancement as well as NG cost savings in a MR compared to a conventional PBR.

Keywords: Ammonia Decomposition, Membrane Reactor, Process Simulation, Hydrogen, PEM Fuel Cells

## INTRODUCTION

Most of world's energy supply primarily depends on fossil fuels like petroleum, natural gas, and coal [1,2]. The increased use of fossil fuels due to industrialization and urbanization has led to sharp increases in air pollution and anthropogenic greenhouse gas emissions. Even with strict environmental regulations, it is inevitable to have air pollution such as CO, $CO_2$, $NO_X$, $SO_2$ and $NH_3$ released to the atmosphere, thus resulting in global warming, acid precipitation, and many serious human health issues [3,4]. Therefore, there is a strong demand for clean energy to meet high energy needs and strict environmental regulations simultaneously.

Fuel cells are a clean and high-efficiency devices that convert chemical energy obtained from either hydrogen or other fuels like methanol and ethanol into electrical energy with only $H_2O$ as a by-product [5-7]. Many researchers have investigated various fuel cells, including proton exchange membrane fuel cells (PEMFCs) [8-15], solid oxide fuel cells (SOFCs) [16-18], molten carbonate fuel cells (MCFCs) [19-21], phosphoric acid fuel cells (PAFCs) [22-24], and alkaline fuel cells (AFCs) [25,26] so far. Among them, PEMFCs are operated with hydrogen as fuel over dissociation of hydrogen to proton followed by reacting with $O_2$ to produce $H_2O$ and electricity. They have several advantages of fewer corrosion problems [8,12], a more compact size [9,10,12], and low operating temperature, enabling a faster start-up [9,11,12] compared to other fuel cells. Therefore, it is extremely important to develop an environmentally friendly process to produce enough hydrogen to be used as a fuel for PEMFCs that can possibly replace current steam methane reforming using fossil fuels for hydrogen production.

Currently, the most widely used route of hydrogen production is steam methane reforming [27-29], and it accounts for nearly 48% of a worldwide hydrogen production [30,31]. However, $CO_2$ is emitted from steam methane reforming and this requires the use of a post treatment unit to capture the produced $CO_2$. To resolve this problem associated with steam methane reforming, several studies have focused on ammonia ($NH_3$) decomposition to produce $CO_X$-free hydrogen, thus eliminating the use of an additional $CO_2$ capture unit and serving as an environmentally friendly process for hydrogen production. In addition, the $CO_X$-free hydrogen can be used as fuel to PEMFCs, limiting CO content less than 10 ppm in a feed stream to avoid catalyst poisoning [32-35]. Ammonia has a higher hydrogen density of 120 kg $m^{-3}$ compared with liquefied hydrogen's density of 70 kg $m^{-3}$ and is believed to cost less than reforming of hydrocarbons to produce hydrogen [36-38]. Moreover, an ammonia decomposition process to produce $H_2$ is free of coking by carbonaceous materials frequently encountered in hydrocarbon reforming [36,38-42]. Previously, decomposition of ammonia was studied to remove trace of toxic ammonia from a coal gasification [43-45]; however, recently many researchers have reported the application of a membrane reactor (MR), a new reactor type combining a reactor and a separator in one unit, to ammonia decomposition for improved hydrogen production by *Le Chatelier*'s principle and possible cost savings due to the compact design. Li et al. [41] carried out experimental work with a novel bimodal catalytic MR consisting of a Ru/$\gamma$-$Al_2O_3$/$\alpha$-$Al_2O_3$ bimodal catalytic support and silica separation membranes and reported enhanced $NH_3$ conversions in a MR. Abashar [42] conducted numerical simulation with multi-stage MRs from 873 K to 1,273 K and reported

†To whom correspondence should be addressed.
E-mail: hklim@cu.ac.kr

that the multi-stage configuration is a good candidate for on-site ultra-clean hydrogen production. Rahimpour and Asgari [43] performed mathematical simulation for hydrogen perm-selective MR using purge gases from an ammonia plant to investigate effect of pressure, temperature, thickness of Pd-Ag catalytic membrane layer, and sweep gas flow ratio on the performance of a MR. García-García et al. [46] performed low temperature ammonia decomposition over Ru-carbon catalyst in an MR fitted with a Pd membrane, and reported improved performance in an MR exceeding thermodynamic equilibrium. Rizzuto et al. [47] also investigated the performance of ammonia decomposition in a catalytic membrane reactor using Ru catalysts and Pd-coated membranes and presented experimental data with ammonia conversion yield of >99.4% at 5 bar and 400 °C. Furthermore, this MR system was proposed as *in-situ* hydrogen production. Itoh et al. [48] carried out both experimental and simulation studies for ammonia decomposition in a palladium MR using an Ru supported catalyst and reported 15% increase in ammonia conversion in an MR compared to a conventional packed-bed reactor (PBR). Further enhancement was expected with a thinner palladium membrane based on their simulation. Carlo et al. [49] performed 2-D and 3-D computational fluid dynamics (CFD) studies for ammonia decomposition over an $Ni/Al_2O_3$ catalyst in an MR fitted with Pd-based membranes and reported that an operating temperature of 550 °C was the most suitable for a reactor in their study. By employing an MR, about 18% increase in ammonia conversion was obtained at 550 °C.

However, most of their work was focused mainly on improved reactant conversions and/or product yields in MRs and rarely on the feasibility studies of ammonia decomposition in a MR to produce a $CO_X$-free hydrogen for PEMFCs, to the best of our knowledge. Therefore, our aim was to evaluate ammonia decomposition in an MR for a $CO_X$-free hydrogen production to be used as a fuel for PEM fuel cells. With this MR technology for ammonia decomposition, several benefits of no coke formation, no $CO_2$ emission, higher hydrogen density, and improved reactant conversion and product yield due to *Le Chatelier*'s principle can be expected. Based on process simulation works using Aspen HYSYS®, parametric studies to investigate the effect of key operating parameters like $H_2$ permeance, sweep gas flow rate, and operating temperature were conducted for a PBR and an MR. All reaction conditions were the same for both reactors except the use of $H_2$ separation membranes in an MR. In addition, costs of natural gas used in a boiler were compared for a PBR and an MR as a preliminary economic study.

## METHODS

### 1. Ammonia Decomposition in a Membrane Reactor (MR) for PEM Fuel Cells

A schematic of ammonia decomposition in an MR and its application to PEM fuel cells is presented in Fig. 1. Ammonia is one of the most produced inorganic chemicals worldwide (more than 100 million ton per year) and is used to manufacture commercial products such as medicines, explosives, and fertilizers [50-53]. In the presence of good supply of a produced ammonia, it can be used to gain hydrogen, which can be used in wide range of industrial applications. In a reaction zone, high-pressure ammonia is fed to an MR filled with catalysts and equipped with $H_2$ separation membranes. In the MR, hydrogen is continuously removed from a shell side of the MR (retentate) and penetrated to a tube side of the MR (permeate) driven by $H_2$ partial pressure difference between a retentate and a permeate. This initiates an equilibrium shift by *Le Chatelier*'s principle leading to improved hydrogen production in an

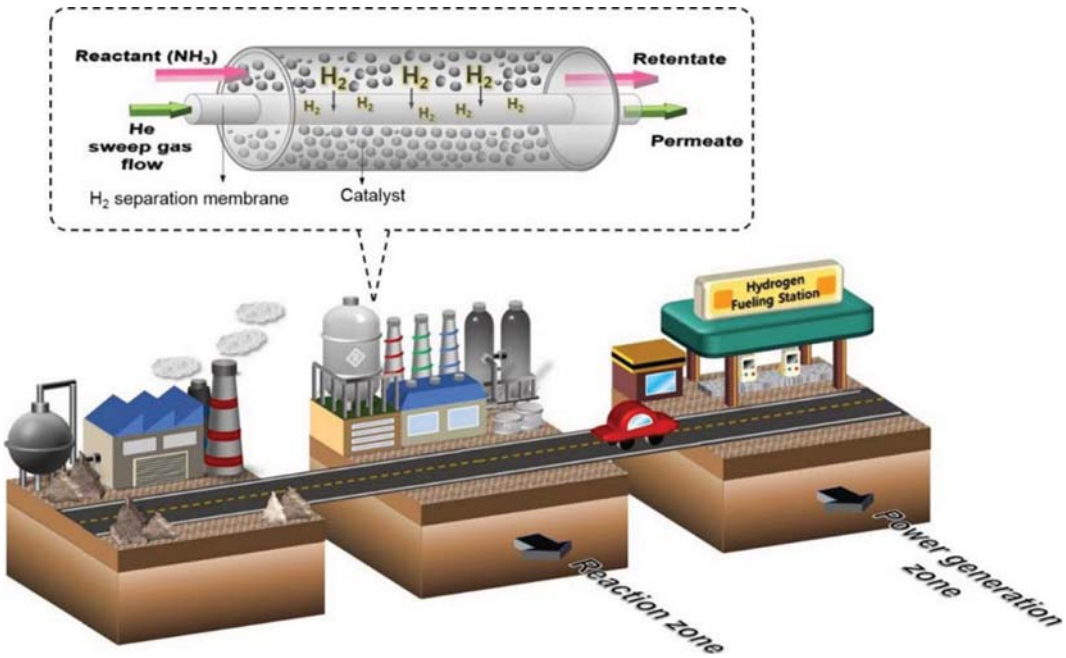


**Fig. 1. Schematic diagram for ammonia decomposition in a membrane reactor (MR) for PEM fuel cells (PEMFCs).**

MR compared to a conventional PBR. Purified hydrogen produced from the permeate side of an MR can be used for wide industrial applications or directly for PEMFCs in a power generation zone only producing $H_2O$ free of CO, $CO_2$, and $NO_X$ [40,43,44].

## 2. Process Simulation Using Aspen HYSYS®

### 2-1. Model Validation

In this study, kinetics of ammonia decomposition (Eqs. (1)-(4)) reported by Temkin and Pyzhev [54] was employed to simulate a PBR and an MR.

$$2NH_3 \rightarrow N_2 + 3H_2 \ (\Delta H_{298} = 46.02 \text{ kJ/mol}) \quad (1)$$

$$r_{NH_3} = k\left[K_{eq}^2 f_{N_2}\left(\frac{f_{H_2}^3}{f_{NH_3}^2}\right)^{1-\beta} - \left(\frac{f_{NH_3}^2}{f_{H_2}^3}\right)^{\beta}\right] \quad (2)$$

$$k = 1.09 \times 10^{20} \exp\left(-\frac{230400}{RT}\right) \quad (3)$$

$$K_{eq} = 2.56 \times 10^{-12} \exp\left(\frac{59031.89}{RT}\right) \quad (4)$$

Steady-state and isothermal conditions were assumed and Peng-Robinson equation of state was chosen as a proper thermodynamic fluid package in this study. The simulated data obtained from using Aspen HYSYS® based on the Temkin and Pyzhev's kinetics were compared with experimental ones using a supported $Ni/Al_2O_3$

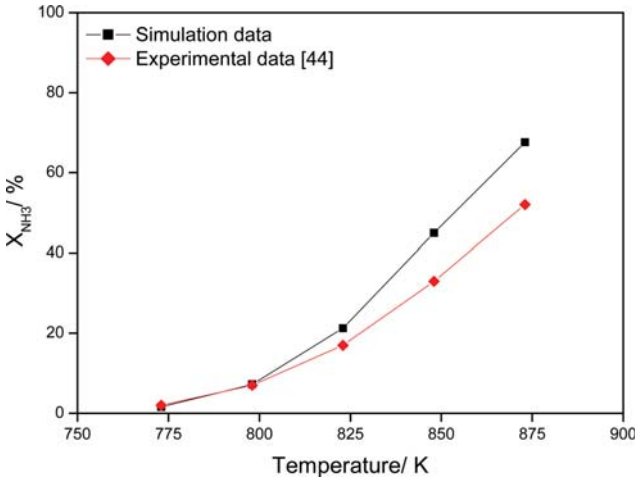


**Fig. 2. Simulation model validation with experimental data.**

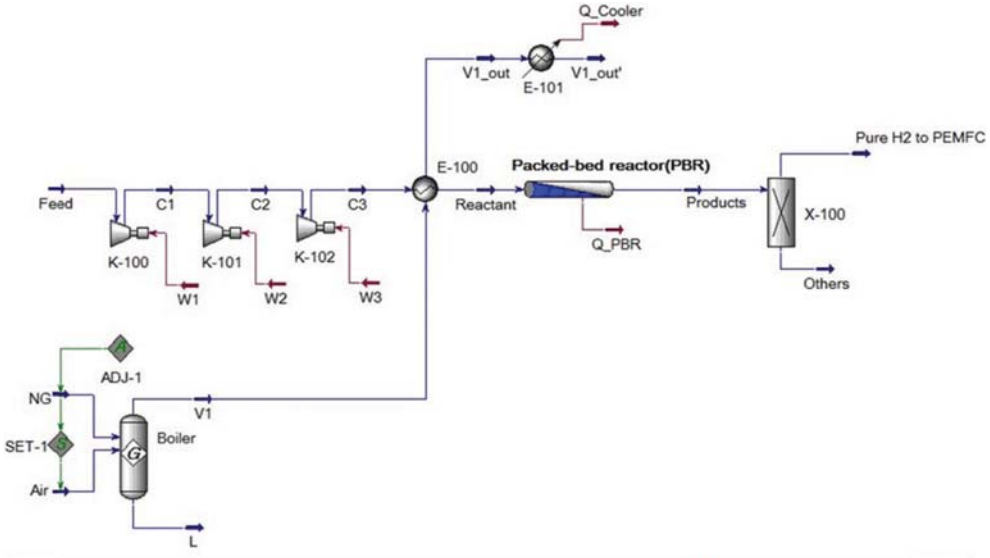


| Stream name | Feed | Reactant | Products | Pure H2 to PEMFC | NG | Air |
|---|---|---|---|---|---|---|
| Pressure/ bar | 1.013 | 16.18 | 16.18 | 16.18 | 1.013 | 1.013 |
| Temperature/ K | 298 | 773 | 773 | 773.5 | 298 | 298 |
| Molar flow/ kmol $h^{-1}$ | 0.9467 | 0.9467 | 1.177 | 0.3448 | 0.0251 | 0.2874 |
| Mass flow/ kg $h^{-1}$ | 16.12 | 16.12 | 16.12 | 0.6951 | 0.4034 | 8.291 |
| Component mole fraction | | | | | | |
| Ammonia | 1.0000 | 1.0000 | 0.6093 | 0.0000 | 0.0000 | 0.0000 |
| Hydrogen | 0.0000 | 0.0000 | 0.2930 | 1.0000 | 0.0000 | 0.0000 |
| Nitrogen | 0.0000 | 0.0000 | 0.0977 | 0.0000 | 0.0000 | 0.7900 |
| Oxygen | 0.0000 | 0.0000 | 0.0000 | 0.0000 | 0.0000 | 0.2100 |
| Methane | 0.0000 | 0.0000 | 0.0000 | 0.0000 | 1.0000 | 0.0000 |
| CO2 | 0.0000 | 0.0000 | 0.0000 | 0.0000 | 0.0000 | 0.0000 |
| CO | 0.0000 | 0.0000 | 0.0000 | 0.0000 | 0.0000 | 0.0000 |
| Helium | 0.0000 | 0.0000 | 0.0000 | 0.0000 | 0.0000 | 0.0000 |

**Fig. 3. Process flow diagram (PFD) and material streams for ammonia decomposition in a PBR connected to PEMFCs.**

catalyst at 773-873 K reported by Collins and Way [44] as shown in Fig. 2. A good agreement between simulation and experimental data was observed with an average deviation of about 6.5% showing large deviations at high temperatures, possibly due to the assumptions made in the simulation (0.4, 0.2, 4.2, 12.0, and 15.6% deviation at 773, 798, 823, 848, and 873 K, respectively). Therefore, a process simulation model developed using Aspen HYSYS® was extensively used in this study to carry out parametric assessment for key operating conditions in a PBR and an MR.

2-2. Process Flow Diagrams (PFDs) for a PBR and a MR

Process simulation studies were performed for ammonia decomposition in both a PBR and an MR using Aspen HYSYS® (Aspen Technology, Inc.), one of the most widely used chemical process simulators [55-59]; respective process flow diagrams (PFDs) and material streams for a PBR and an MR are depicted in Fig. 3 and Fig. 4. An MR process model was created with a template including a series of plug flow reactors and component splitters based on previous studies [60-63], because it does not exist in the interface of Aspen HYSYS®. With the proposed process models, parametric studies to compare the performance of a PBR and a MR were carried out. To provide required heat for the reaction, a boiler was used by burning natural gas with 20% excess oxygen. Reaction conditions and membrane properties are presented in Table 1. $H_2$ separation membranes employed in this study were assumed to have infinite selectivity. Based on process simulation results, preliminary economic analysis was conducted to assess possible cost savings in an MR compared to a PBR, reflecting a current natural gas (NG) price obtained from Korea Gas Corporation (KOGAS), which is considered as one of the critical economic factors.

**Table 1. Reaction conditions and membrane properties**

| | | |
|---|---|---|
| Reactant | $NH_{3\ in}$/kmol $h^{-1}$ | 0.9467 |
| Reactor (PBR/MR) | Temperature/K | 773-873 |
| | Catalyst density/kg $m^{-3}$ | 970 |
| | Void fraction | 0.4 |
| | Length/cm | 30 |
| | Diameter/cm | 10 |
| | GHSV*/$h^{-1}$ | 10000 |
| $H_2$ separation membrane | Length/cm | 30 |
| | Diameter/cm | 1 |
| | Number of membrane tubes | 10 |
| | $H_2$ permeance/mol $m^{-2}$ $s^{-1}$ $Pa^{-1}$ | $1\times10^{-6}$~$6\times10^{-6}$ |
| | $H_2$ selectivity | Infinite |

*Gas hourly space velocity

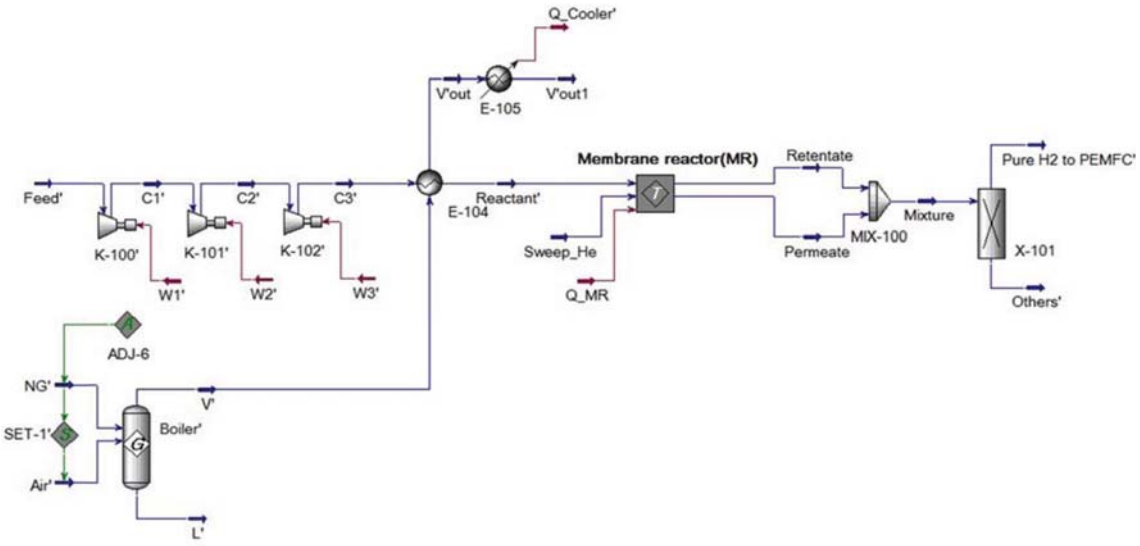


| Stream name | Feed' | Reactant' | Sweep_He | Retentate | Pure H2 to PEMFC' | Permeate | NG' | Air' |
|---|---|---|---|---|---|---|---|---|
| Pressure/ bar | 1.013 | 16.18 | 1.013 | 16.18 | 1.013 | 1.013 | 1.013 | 1.013 |
| Temperature/ K | 298 | 773 | 298 | 773 | 629.5 | 368.5 | 298 | 298 |
| Molar flow/ kmol $h^{-1}$ | 0.9467 | 0.9467 | 5 | 0.773 | 0.3893 | 5.617 | 0.0404 | 0.462 |
| Mass flow/ kg $h^{-1}$ | 16.12 | 16.12 | 20.01 | 14.88 | 0.7848 | 21.26 | 0.6485 | 13.33 |
| Component mole fraction | | | | | | | | |
| Ammonia | 1.0000 | 1.0000 | 0.0000 | 0.6514 | 0.0000 | 0.0000 | 0.0000 | 0.0000 |
| Hydrogen | 0.0000 | 0.0000 | 0.0000 | 0.0620 | 1.0000 | 0.1098 | 0.0000 | 0.0000 |
| Nitrogen | 0.0000 | 0.0000 | 0.0000 | 0.2867 | 0.0000 | 0.0000 | 0.0000 | 0.7900 |
| Oxygen | 0.0000 | 0.0000 | 0.0000 | 0.0000 | 0.0000 | 0.0000 | 0.0000 | 0.2100 |
| Methane | 0.0000 | 0.0000 | 0.0000 | 0.0000 | 0.0000 | 0.0000 | 1.0000 | 0.0000 |
| CO2 | 0.0000 | 0.0000 | 0.0000 | 0.0000 | 0.0000 | 0.0000 | 0.0000 | 0.0000 |
| CO | 0.0000 | 0.0000 | 0.0000 | 0.0000 | 0.0000 | 0.0000 | 0.0000 | 0.0000 |
| Helium | 0.0000 | 0.0000 | 1.0000 | 0.0000 | 0.0000 | 0.8902 | 0.0000 | 0.0000 |

**Fig. 4. Process flow diagram (PFD) and material streams for ammonia decomposition in a MR connected to PEMFCs.**

## RESULTS AND DISCUSSION

### 1. Effect of He Sweep Gas Flow, $H_2$ Permeance, and Operating Temperature

Aspen HYSYS®, a commercial chemical process simulator, was used to calculate ammonia conversion ($X_{NH_3}$) enhancement defined as $\frac{X_{NH_3,\,MR}-X_{NH_3,\,PBR}}{X_{NH_3,\,PBR}}\times 100\ (\%)$ and $H_2$ yield enhancement defined as $\frac{H_2\ \text{yield}_{,\,MR}-H_2\ \text{yield}_{,\,PBR}}{H_2\ \text{yield}_{,\,PBR}}\times 100\ (\%)$ in an MR compared to a PBR by employing kinetics reported by Temkin and Pyzhev [54]. In this study, pure helium was used as a sweep gas, which was passed through the permeate side of an MR. Generally, inert gases such as $N_2$, Ar, and He are used as a sweep gas [64-67] to drive increased partial pressure difference of hydrogen between a retentate and a permeate in an MR [68-72].

Fig. 5 shows the effect of key operating parameters, He sweep gas flow, $H_2$ permeance, and operating temperature, on the ammonia conversion ($X_{NH_3}$) enhancement in an MR compared with a PBR. First, there was a general trend of increased $X_{NH_3}$ enhancement in an MR with increased $H_2$ permeance and He sweep gas flow, but decreased operating temperature. Interestingly, there are some noteworthy results for He sweep gas flow. First, it was clearly observed that the effect of He sweep gas was positive, showing improved $X_{NH_3}$ enhancement for all conditions studied here compared to one with no sweep gas, and this confirms the necessity of employing a sweep gas to drive $H_2$ partial pressure difference between a retentate and a permeate in an MR further. Second, the effect of He sweep gas flow was significant at lower operating temperatures,

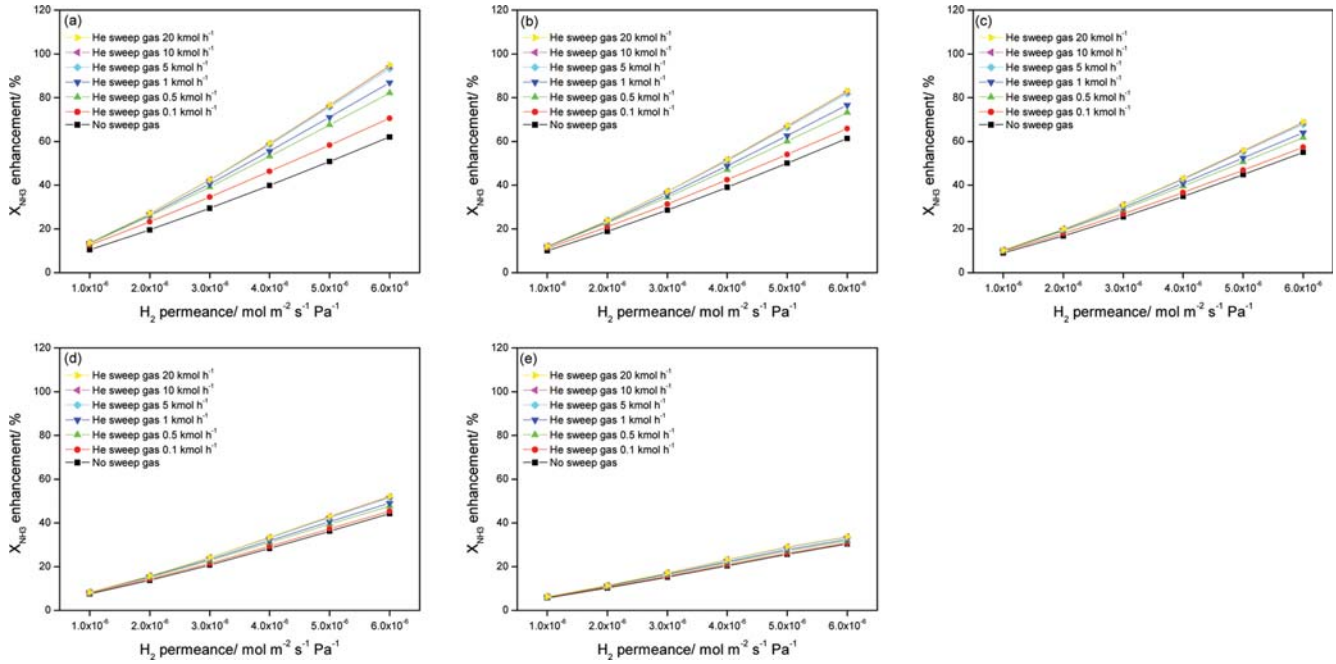


**Fig. 5. Effect of a He sweep gas flow rate and a $H_2$ permeance on an ammonia conversion ($X_{NH_3}$) enhancement in a MR at (a) 773 K, (b) 798 K, (c) 823 K, (d) 848 K, and (e) 873 K.**

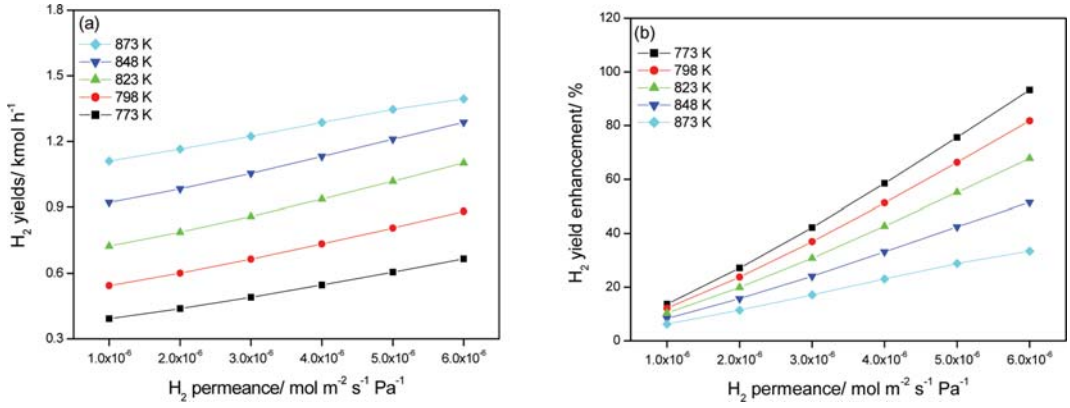


**Fig. 6. Effect of a $H_2$ permeance on (a) a $H_2$ yield and (b) a $H_2$ yield enhancement at 773-873 K in a MR with a fixed He sweep gas flow rate of 5 kmol $h^{-1}$.**

while it became trivial as operating temperatures increased. Therefore, it is reasonable to maintain operating temperature lower in an MR to gain benefits of lower capital and operating costs of a reactor as well as more favorable effect of He sweep gas. Last, there existed a critical point (~5 kmol $h^{-1}$) above which no further effect of He sweep gas flow was observed, and this value should be taken into account to avoid any unnecessary supply of an additional He sweep gas flow. Conclusively, these results provide comprehensive design guidelines to be used for an MR efficiently and economically.

Based on a critical He sweep gas flow rate of 5 kmol $h^{-1}$, the effect of $H_2$ permeance on $H_2$ yield (Fig. 6(a)) and $H_2$ yield enhancement (Fig. 6(b)) at 773-873 K in an MR was investigated. Apparently, a higher $H_2$ permeance resulted in a higher $H_2$ yield and $H_2$ yield enhancement, and this necessitates the use of $H_2$ membranes having a higher $H_2$ permeance such as Pd membranes to take full advantage of an MR [73-75]. Compared to respective $H_2$ yields of 0.35, 0.49, 0.66, 0.85, and 1.05 kmol $h^{-1}$ at temperatures of 773, 798, 823, 848, and 873 K in a PBR, enhanced $H_2$ yields were observed in an MR for all temperatures studied as shown in Fig. 6(a). In addition, a higher $H_2$ yield was obtained at a higher temperature due to the endothermic nature of ammonia decomposition. However, if $H_2$ yield enhancement ($\frac{H_2\ \text{yield}_{,MR} - H_2\ \text{yield}_{,PBR}}{H_2\ \text{yield}_{,PBR}} \times 100\ (\%)$) is considered, a higher $H_2$ yield enhancement was observed at a lower temperature showing a reverse effect of temperature on $H_2$ yield enhancement contrary to a favorable effect of temperature on $H_2$ yield. It seems that there is less room for improvement in $H_2$ yield at high temperatures in an MR compared to a PBR (6-33% at 873 K vs 14-93% at 773 K), because a relatively high $H_2$ yield is already obtained in a PBR at high temperatures due to the endothermicity of ammonia decomposition.

**2. Cost Estimation for Natural Gas (NG) Usage in a Boiler**

As a preliminary economic analysis for a PBR and an MR, cost estimations for NG usage in a boiler were performed based on NG amounts required to supply heat for a PBR and an MR. A fixed $H_2$ permeance of $6\times10^{-6}$ mol $m^{-2}$ $s^{-1}$ and a He sweep gas flow rate

**Table 2. Comparative studies for a PBR and a MR with a $H_2$ permeance of $6\times10^{-6}$ mol $m^{-2}$ $s^{-1}$ $Pa^{-1}$ and a He sweep gas flow rate of 5 kmol $h^{-1}$ at 773 K**

| | $X_{NH_3}$/% | Produced $H_2$ yield/kmol $h^{-1}$ | NG in a boiler/kmol $h^{-1}$ | NG operating cost in a boiler/\$ $y^{-1}$ |
|---|---|---|---|---|
| Packed-bed reactor (773 K) | 24.28 | 0.3448 | $2.51\times10^{-2}$ | 1970.84 |
| Membrane reactor (773 K) | 46.82 | 0.6648 | $4.04\times10^{-2}$ | 3268.59 |
| Membrane reactor (753 K) | 36.05 | 0.5119 | $3.18\times10^{-2}$ | 2490.81 |
| Membrane reactor (733 K) | 26.92 | 0.3823 | $2.43\times10^{-2}$ | 1904.13 |
| Membrane reactor (713 K) | 19.53 | 0.2773 | $1.80\times10^{-2}$ | 1412.70 |
| Membrane reactor (726.4 K) | 24.28 | 0.3448 | $2.21\times10^{-2}$ | 1730.79 |
| | | | Reduction/% | 12.18 |

**Table 3. Comparative studies for a PBR and a MR with a $H_2$ permeance of $6\times10^{-6}$ mol $m^{-2}$ $s^{-1}$ $Pa^{-1}$ and a He sweep gas flow rate of 5 kmol $h^{-1}$ at 823 K**

| | $X_{NH_3}$/% | Produced $H_2$ yield/kmol $h^{-1}$ | NG in a boiler/kmol $h^{-1}$ | NG operating cost in a boiler/\$ $y^{-1}$ |
|---|---|---|---|---|
| Packed-bed reactor (823 K) | 46.24 | 0.6566 | $4.35\times10^{-2}$ | 3450.14 |
| Membrane reactor (823 K) | 77.46 | 1.0999 | $6.48\times10^{-2}$ | 5140.09 |
| Membrane reactor (803 K) | 65.11 | 0.9246 | $5.50\times10^{-2}$ | 4358.25 |
| Membrane reactor (783 K) | 52.71 | 0.7485 | $4.51\times10^{-2}$ | 3577.86 |
| Membrane reactor (763 K) | 41.24 | 0.5857 | $3.60\times10^{-2}$ | 2852.26 |
| Membrane reactor (772 K) | 46.24 | 0.6566 | $4.00\times10^{-2}$ | 3169.60 |
| | | | Reduction/% | 8.13 |

**Table 4. Comparative studies for a PBR and a MR with a $H_2$ permeance of $6\times10^{-6}$ mol $m^{-2}$ $s^{-1}$ $Pa^{-1}$ and a He sweep gas flow rate of 5 kmol $h^{-1}$ at 873 K**

| | $X_{NH_3}$/% | Produced $H_2$ yield/kmol $h^{-1}$ | NG in a boiler/kmol $h^{-1}$ | NG operating cost in a boiler/\$ $y^{-1}$ |
|---|---|---|---|---|
| Packed-bed reactor (873 K) | 73.61 | 1.0453 | $5.46\times10^{-2}$ | 5223.31 |
| Membrane reactor (873 K) | 98.20 | 1.3945 | $7.56\times10^{-2}$ | 6563.31 |
| Membrane reactor (853 K) | 92.63 | 1.3154 | $6.72\times10^{-2}$ | 6139.62 |
| Membrane reactor (833 K) | 83.17 | 1.1811 | $5.75\times10^{-2}$ | 5507.93 |
| Membrane reactor (713 K) | 71.37 | 1.0135 | $4.75\times10^{-2}$ | 4753.33 |
| Membrane reactor (816.6 K) | 73.61 | 1.0453 | $5.08\times10^{-2}$ | 4894.82 |
| | | | Reduction/% | 6.29 |

of 5 kmol $h^{-1}$ were used for this study. As shown in Table 2, comparative studies to calculate NG amounts and NG operating costs in a boiler were performed at 773 K to obtain the same amount of $H_2$ in both a PBR and an MR, and NG cost reduction of 12.18% was obtained in the MR. Further analysis for 823 and 873 K revealed that similar results were obtained showing respective NG cost reductions of 8.13% at 823 K (Table 3) and 6.29% at 873 K (Table 4) in MRs suggesting implementing an MR at lower temperatures to gain better NG cost reduction.

## CONCLUSIONS

Conceptual design studies of a $CO_x$-free hydrogen production from ammonia decomposition in a membrane reactor (MR) for PEM fuel cells (PEMFCs) were performed based on process simulation models developed and validated by previously reported kinetics and experimental data.

Higher ammonia conversions and $H_2$ yields were obtained in an MR than the ones in a packed-bed reactor (PBR). For $X_{NH_3}$ and $H_2$ yield enhancements, defined as a relative increase in an MR compared to a PBR, He sweep gas flow was positive for $X_{NH_3}$ enhancement in an MR also providing a critical value of 5 kmol $h^{-1}$ above which no further effect was obtained. In addition, the effect was significant at lower temperature with minor at higher temperature. $H_2$ permeance turned out to be positive for $H_2$ yield enhancement in an MR requiring the development of $H_2$ separation membranes with a higher $H_2$ permeance. For the same $H_2$ permeance, lower operating temperature led to higher $H_2$ yield enhancement in an MR. As for cost estimations for natural gas usage, apparent cost reductions were observed in an MR due to increased $H_2$ production, showing more reductions at lower temperatures (12.18, 8.13, and 6.29% at 773, 823, and 873 K, respectively).

## ACKNOWLEDGEMENTS

This work was supported by the Human Resources Program in Energy Technology of the Korea Institute of Energy Technology Evaluation and Planning (KETEP), granted financial resource from the Ministry of Trade, Industry & Energy, Republic of Korea (No. 20174010201330).

## NOMENCLATURE

PEMFCs : proton exchange membrane fuel cells
SOFCs : solid oxide fuel cells
MCFCs : molten carbonate fuel cells
PAFCs : phosphoric acid fuel cells
AFCs : alkaline fuel cells
MR : membrane reactor
PBR : packed-bed reactor
CFD : computational fluid dynamics
k : rate constant of reaction [mol $Pa^{0.674}$ $h^{-3}$ $s^{-1}$]
$K_{eq}$ : equilibrium constant for reaction [$Pa^{-1}$]
$f_i$ : fugacity of species i
PFD : process flow diagram
GHSV : gas hourly space velocity [$h^{-1}$]
NG : natural gas
KOGAS : Korea gas corporation

## REFERENCES

1. F. Dragomir, O. Dragomir, N. Olariu, and A. Oprea, *SBEEF*, **3**, 5 (2013).
2. X. Lu, S. Xie, H. Yang, Y. Tong and H. Ji, *Chem. Soc. Rev.*, **43**, 7581 (2014).
3. M. E. E. Abashar, Y. S. Al-Sughair and I. S. Al-Mutaz, *Appl. Catal. A-Gen.*, **236**, 35 (2002).
4. A. Midilli, *Int. J. Glob. Warm.*, **10**, 354 (2016).
5. Z. Yang, H. Nie, X. Chen, X. Chen and S. Huang, *J. Power Sources*, **236**, 238 (2013).
6. C. Lamy, T. Jaubert, S. Baranton and C. Coutanceau, *J. Power Source*, **245**, 927 (2014).
7. O. Z. Sharaf and M. F. Orhan, *Renew. Sust. Energ. Rev.*, **32**, 810 (2014).
8. R. Sousa and E. R. Gonzalez, *J. Power Source*, **147**, 32 (2005).
9. R. Mohtadi, W.-K. Lee and J. W. Van Zee, *Appl. Catal. B-Environ.*, **56**, 37 (2005).
10. P. Thounthong, S. Raël and B. Davat, *J. Power Source*, **193**, 376 (2009).
11. J. J. Baschuk and X. Li, *Appl. Energy*, **86**, 181 (2009).
12. A. Contreras, F. Posso and E. Guervos, *Appl. Energy*, **87**, 1376 (2010).
13. B. Shabani and J. Andrews, *Int. J. Hydrogen Energy*, **36**, 5442 (2011).
14. F.-C. Wang and Y.-S. Chiang, *Int. J. Hydrogen Energy*, **37**, 11299 (2012).
15. U. Byambasuren, Y. Jeon, D. Altansukh, Y. Ji and Y.-G. Shul, *Korean J. Chem. Eng.*, **33**, 1831 (2016).
16. N. Q. Minh, *Solid State Ion.*, **174**, 271 (2004).
17. D. J. L. Brett, A. Atkinson, N. P. Brandon and S. J. Skinner, *Chem. Soc. Rev.*, **37**, 1568 (2008).
18. A. J. Jacobson, *Chem. Mat.*, **22**, 660 (2010).
19. A. L. Dicks, *Curr. Opin. Solid State Mat. Sci.*, **8**, 379 (2004).
20. J. Brouwer, F. Jabbari, E. M. Leal and T. Orr, *J. Power Source*, **158**, 213 (2006).
21. T.-Y. Kim, B.-S. Park and Y.-K. Yeo, *Korean J. Chem. Eng.*, **34**, 1952 (2017).
22. R.-H. Song, C.-S. Kim and D. R. Shin, *J. Power Source*, **86**, 289 (2000).
23. M. Neergat and A. K. Shukla, *J. Power Source*, **102**, 317 (2001).
24. N. Sammes, R. Bove and K. Stahl, *Curr. Opin. Solid State Mat. Sci.*, **8**, 372 (2004).
25. E. Gülzow, *J. Power Source*, **61**, 99 (1996).
26. K. Kordesch, V. Hacker, J. Gsellmann, M. Cifrain, G. Faleschini, P. Enzinger, R. Fankhauser, M. Ortner, M. Muhr and R. R. Aronson, *J. Power Source*, **86**, 162 (2000).
27. B. Bej, N. C. Pradhan and S. Neogi, *Catal. Today*, **207**, 28 (2013).
28. T. L. LeValley, A. R. Richard and M. Fan, *Int. J. Hydrogen Energy*, **39**, 16983 (2014).
29. M. Nawfal, C. Gennequin, M. Labaki, B. Nsouli, A. Aboukaïs and E. Abi-Aad, *Int. J. Hydrogen Energy*, **40**, 1269 (2015).
30. A. Ursua, L. M. Gandia and P. Sanchis, *Proc. IEEE*, **100**, 410 (2012).
31. M. Voldsund, K. Jordal and R. Anantharaman, *Int. J. Hydrogen Energy*, **41**, 4969 (2016).

32. C. Song, *Catal. Today*, **77**, 17 (2002).
33. Y.-T. Seo, D.-J. Seo, J.-H. Jeong and W.-L. Yoon, *J. Power Source*, **160**, 505 (2006).
34. Y.-H. Kim, E.-D. Park, H.-C. Lee and D. Lee, *Appl. Catal. A-Gen.*, **366**, 363 (2009).
35. E.-D. Park, D. Lee and H.-C. Lee, *Catal. Today*, **139**, 280 (2009).
36. R.-Y. Chein, Y.-C. Chen, C.-S. Chang and J. N. Chung, *Int. J. Hydrogen Energy*, **35**, 589 (2010).
37. A.-H. Lu, J.-J. Nitz, M. Comotti, C. Weidenthaler, K. Schlichte, C. W. Lehmann, O. Terasaki and F. Schüth, *J. Am. Chem. Soc.*, **132**, 14152 (2010).
38. M. Miyamoto, R. Hayakawa, Y. Makino, W. Oumi, S. Uemiya and M. Asanuma, *Int. J. Hydrogen Energy*, **39**, 10154 (2014).
39. A. D. Carlo, L. Vecchione and Z. D. Prete, *Int. J. Hydrogen Energy*, **39**, 808 (2014).
40. G. Li, M. Kanezashi, T. Yoshioka and T. Tsuru, *AIChE J.*, **59**, 168 (2013).
41. G. Li, M. Kanezashi, H. R. Lee, M. Maeda, T. Yoshioka and T. Tsuru, *Int. J. Hydrogen Energy*, **37**, 12105 (2012).
42. M. E. E. Abashar, *J. King Saud Univ., Eng. Sci.* (2016), DOI:10.1016/j.jksues.2016.01.002.
43. M. R. Rahimpour and A. Asgari, *Int. J. Hydrogen Energy*, **34**, 5795 (2009).
44. J. P. Collins and J. D. Way, *J. Membr. Sci.*, **96**, 259 (1994).
45. A. Chambers, Y. Yoshii, T. Inada and T. Miyamoto, *Can. J. Chem. Eng.*, **74**, 929 (1996).
46. F. R. García-García, Y. H. Ma, I. Rodríguez-Ramos and A. Guerrero-Ruiz, *Catal. Commun.*, **9**, 482 (2008).
47. E. Rizzuto, P. Palange and Z. D. Prete, *Int. J. Hydrogen Energy*, **39**, 11403 (2014).
48. N. Itoh, A. Oshima, E. Suga and T. Sato, *Catal. Today*, **236**, 70 (2014).
49. A. D. Carlo, A. Dell'Era and Z. D. Prete, *Int. J. Hydrogen Energy*, **36**, 11815 (2011).
50. H. Jasuja, G. W. Peterson, J. B. Decoste, M. A. Browe and K. S. Walton, *Chem. Eng. Sci.*, **124**, 118 (2015).
51. F. Vitse, M. Cooper and G. G. Botte, *J. Power Source*, **142**, 18 (2005).
52. I. A. Amar, R. Lan, C. T. G. Petit and S. Tao, *J. Solid State Electochem.*, **15**, 1845 (2011).
53. J. M. Modak, *Resonance*, **16**, 1159 (2011).
54. M. I. Temkin and V. Pyzhev, *Acta Phys. Chim. URSS*, **12**, 217 (1940).
55. A. H. West, D. Posarac and N. Ellis, *Bioresour. Technol.*, **99**, 6587 (2008).
56. M. Bassyouni, S. W. ul Hasan, M. H. Abdel-Aziz, S. M.-S. Abdelhamid, S. Naveed, A. Hussain and F. N. Ani, *Energy Convers. Manage.*, **88**, 693 (2014).
57. L. E. Øi, T. Bråthen, C. Berg, S. K. Brekne, M. Flatin, R. Johnsen, I. G. Moen and E. Thomassen, *Energy Procedia*, **51**, 224 (2014).
58. B. Lee, S. Lee, H. Y. Jung, S.-K. Ryi and H. Lim, *Front. Chem. Sci. Eng.*, **10**, 224 (2014).
59. B. Lee, S. Jeong, S. Lee, H.-Y. Jung, S.-K. Ryi and H. Lim, *Greenh. Gases*, **7**, 542 (2017).
60. A. Sarvar-Amini, R. Sotudeh-Gharebagh, H. Bashiri, N. Mostoufi and A. Haghtalab, *Energy Fuels*, **21**, 3593 (2007).
61. M. Roberts, R. Zabransky, S. Doong and J. Lin, *Single membrane reactor configuration for separation of hydrogen, carbon dioxide and hydrogen sulfide*, Department of Energy, U.S.A. (2008).
62. S. Jeong, S. Kim, B. Lee, S.-K. Ryi and H. Lim, *Int. J. Hydrogen Energy* (2017), DOI:10.1016/j.ijhydene.2017.07.202.
63. S. Kim, S.-K. Ryi and H. Lim, *Int. J. Hydrogen Energy* (2017), DOI: 10.1016/j.ijhydene.2017.09.084.
64. P. Zeng, Z. Chen, W. Zhou, H. Gu, Z. Shao and S. Liu, *J. Membr. Sci.*, **291**, 148 (2007).
65. D. Mendes, V. Chibante, J.-M. Zheng, S. Tosti, F. Borgognoni, A. Mendes and L. M. Madeira, *Int. J. Hydrogen Energy*, **35**, 12596 (2010).
66. M. P. Lobera, J. M. Serra, S. P. Foghmoes, M. Søgaard and A. Kaiser, *J. Membr. Sci.*, **385-386**, 154 (2011).
67. A. Santos, J. Coronas, M. Menéndez and J. Santamaría, *Catal. Lett.*, **30**, 189 (1994).
68. M. B. Rao and S. Sircar, *J. Membr. Sci.*, **110**, 109 (1996).
69. P. Ferreira-Aparicio, M. Benito, K. Kouachi and S. Menad, *J. Catal.*, **231**, 331 (2005).
70. S. Bhatia, C. Y. Thien and A. R. Mohamed, *Chem. Eng. J.*, **148**, 525 (2009).
71. W. Yu, T. Ohmori, T. Yamamoto, A. Endo, M. Nakaiwa, T. Hayakawa and N. Itoh, *Int. J. Hydrogen Energy*, **30**, 1071 (2005).
72. B. Lee and H. Lim, *Korean J. Chem. Eng.*, **34**, 199 (2017).
73. E. Kikuchi, *Catal. Today*, **56**, 97 (2000).
74. H. Lim and S. T. Oyama, *J. Membr. Sci.*, **378**, 179 (2011).
75. M. R. Rahimpour, F. Samimi, A. Babapoor, T. Tohidian and S. Mohebi, *Chem. Eng. Process.*, **121**, 24 (2017).